International Journal of Heat and Technology
Vol. 43, No. 2, April, 2025, pp. 493-501
Journal homepage: http://iieta.org/journals/ijht

# Spatial Propagation of Pressure Waves in a Liquid During Electrical Discharge

Oleksiy Smirnov[1], Iurii Dolganov[2*], Oleh Khvoshchan[1], Bohdan Lychko[3], Oleksandr Melnyk[4], Iryna Vorchakova[5]

[1] Department of Impulse Processes of Energy Conversion and Methods and Technologies of Processing Non-Metallic Materials, Institute of Pulse Processes and Technologies of NAS of Ukraine, Mykolaiv 54018, Ukraine
[2] Faculty of Science, Technology and Medicine, Department of Engineering, University of Luxembourg, Luxembourg L-1359, Luxembourg
[3] Department of Ship Power Plants Operation and Thermal Power Engineering, Admiral Makarov National University of Shipbuilding, Mykolaiv 54007, Ukraine
[4] Department of Law and Information Technologies, Separate Structural Subdivision of Higher Education Institution, Open International University of Human Development "Ukraine", Mykolaiv 54003, Ukraine
[5] Department of Translation, Admiral Makarov National University of Shipbuilding, Mykolaiv 54007, Ukraine

Corresponding Author Email: iurii.dolganov@uni.lu



https://doi.org/10.18280/ijht.430211

**Received:** 27 February 2025
**Revised:** 11 April 2025
**Accepted:** 25 April 2025
**Available online:** 30 April 2025

***Keywords:***
*high-voltage electrical discharge, fluid dynamics, pressure wave propagation, numerical modeling, semi-empirical model*

**ABSTRACT**

This study investigates the spatial propagation of pressure waves in a liquid during high-voltage electrical discharge (HVED) using numerical modeling and semi-empirical expressions. It is found that the amplitude of the pressure wave in the equatorial plane of the discharge channel decreases according to a power law, which is in good agreement with previously obtained results. The pressure distribution along the normal, drawn to the equatorial plane of the channel discharge, can be represented by a power dependence. In this case, the exponent decreases with the direction of the distance from the source of disturbance in the equatorial plane. A comparison of the results of mathematical modeling and experiments showed satisfactory agreement. The main limitations of the model include neglect of the viscosity of the liquid. The novelty of this study lies in the simultaneous use and direct comparison of two fundamentally different modeling approaches-a semi-empirical method and a numerical simulation-for assessing pressure wave propagation in both equatorial and non-equatorial planes. The obtained dependences can be used to assess the efficiency of electric discharge action on an object with a known tensile strength at any point in the working space.

## 1. INTRODUCTION

Electrical explosion HVED in a liquid, specifically the breakdown of a liquid gap between electrodes due to the application of high voltage to one of them, has found wide application as a source of pressure waves [1, 2] in various practical applications (Figure 1) [3-8].

- Processing various raw materials of plant origin, including the extraction of various acids from them.
- Destruction and crushing of non-metallic materials - the shock wave generated by HVED can be used to break rocks and minerals, crush brittle materials, and break concrete structures.
- Medical applications - controlled shock waves can be used in medical procedures to break up kidney stones.
- Cleaning of water and oil wells-pressure waves break up sediments that prevent fluid from entering the well.
- Underwater shock wave research-HVED is used to study the behavior of shock waves in liquids, modeling explosive effects.
- Water purification from biological and chemical contaminants, and many other areas of practical application.

Most of the technologies that HVED can be called discharge-pulse technologies (DPT). DPT has several advantages. The main ones are:

- High efficiency of impact;
- Environmental friendliness;
- The possibility of regulating the impact parameters;
- Relatively low cost of equipment and ease of implementation of impact.

Briefly, the physical essence of HVED can be described as follows. During HVED, a high energy density forms in a specific volume (the discharge channel) within a short time, leading to a sharp increase in pressure and temperature. This results in the rapid expansion of the discharge channel, emitting a pressure wave into the surrounding medium [9]. In many DPT, the pressure wave is the key factor determining the effectiveness of the process.

Therefore, all works aimed at increasing the efficiency of the DPT by studying the generated pressure wave are relevant and have practical and scientific value.

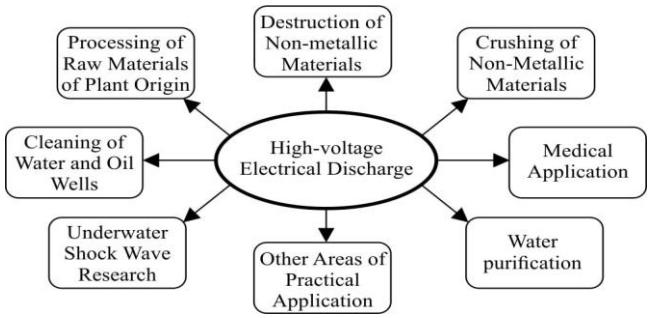


**Figure 1.** Some examples of HVED practical applications

Of particular interest are the studies on the propagation of the pressure wave and the determination of its main parameters (for example, amplitude) at any point in the working space. These studies allow us to predict the effectiveness of the impact, determine the effective parameters of the DPT equipment at the design stage, and determine the limits of the applicability of the DPT.

Although numerous studies have addressed pressure wave propagation in liquids during HVED, the majority focus exclusively on equatorial planes and often utilize a single modeling approach. The present study addresses this gap by developing and comparing two distinct models-semi-empirical and numerical-to investigate wave behavior both in equatorial and off-plane regions. This comprehensive approach allows for enhanced spatial analysis and contributes novel predictive tools for optimizing DPT in various industrial contexts.

## 2. METHODOLOGY, PURPOSE, AND OBJECTIVES OF THE STUDY

Numerous studies have been dedicated to investigating pressure waves in HVED within liquids [10-19]. The propagation of pressure waves in liquid during HVED was studied directly in the previous studies [13-19].

As the pressure wave generated by HVED propagates from the disturbance source, its temporal profile transforms, increasing in duration while decreasing in amplitude.

At different distances from the source (Figure 2), the highest-pressure wave amplitudes are observed in the equatorial plane of the discharge channel (OA). At points deviating from the equatorial plane by an angle $\varphi$ (point B), the amplitudes are lower.

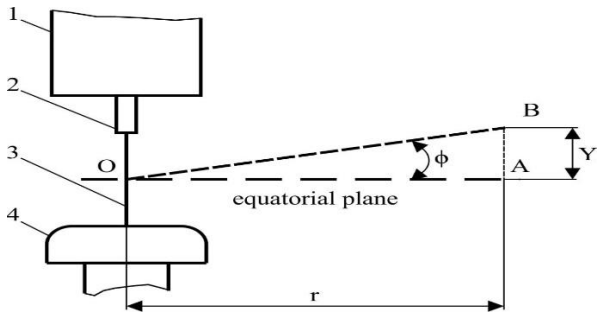


1-Insulator; 2-Electrode (Anode); 3-Discharge channel; 4-Electrode (Cathode); r-Distance from the discharge channel in the equatorial plane (m); Y-Vertical distance from the equatorial plane of the discharge channel to point B (m); φ-Angle between segment OB and the equatorial plane (rad)

**Figure 2.** Spatial scheme of pressure wave propagation during electrical discharge

In the study of Shamko and Kucherenko [13], based on experimental findings, it was suggested that in the equatorial plane of the discharge channel, the pressure wave propagates according to a combined law depending on the distance from the source and the electrode gap length.

At distances less than 2.5l (where l is the interelectrode gap length), the pressure wave amplitude decreases according to a law similar to cylindrical compression waves.

In the range from 2.5l to 5.5l, there is a transition zone from cylindrical to spherical compression waves.

Beyond 5.5l, the propagation follows the law of spherical waves.

In the study of Miyata and Ito [15], it was noted that in the near-field region of the discharge channel, pressure waves propagate with cylindrical symmetry, transitioning to spherical symmetry at greater distances. The study of Liu et al. [16] showed that at distances greater than≈2.5l, the propagation law is closer to that of spherical waves than cylindrical ones. At larger distances (0.4 m to 0.7 m), wave propagation was studied in the research of Chai et al. [17], where the interelectrode gap varied from 5mm to 50mm. It was found that attenuation follows a power-law dependence, with pressure wave amplitudes inversely proportional to distance. At these distances, the generated waves were classified as spherical.

The study of Li et al. [18], which examined conductor explosions (conductor length 80 mm), noted that up to 700 mm from the source, the pressure wave amplitude decreases proportionally to the distance according to the law $r^{-0.74}$.

In the study of Yan et al. [19], it was reported that pressure wave amplitude decay in water can be described by an exponential dependence.

Recent theoretical advancements have furthered our understanding of pressure wave propagation in liquids, particularly in complex media such as bubbly liquids. Kanagawa et al. [20, 21] developed weakly nonlinear theories that account for bubble size distribution and thermal effects within bubbles, offering insights into wave attenuation and dispersion phenomena. Furthermore, Zhang et al. [22] proposed a low-dissipation smoothed-particle hydrodynamics method for modeling pressure wave propagation in weakly compressible fluids. These studies offer complementary perspectives that support the modeling approaches developed in the present work.

Considering the above findings, we assume that during HVED in a liquid, pressure waves propagate in the equatorial plane of the discharge channel with amplitude decay following a power-law dependence (1). At distances less than 2.5l from the discharge channel axis, the pressure wave amplitude decreases according to a cylindrical wave compression law, while beyond 2.5l, it follows a spherical wave compression law.

Accordingly, the amplitude decay law with distance can be expressed as:

$$P_{max} = P_{max00} r^{-k_r} \quad (1)$$

where, $P_{max}$ is the pressure wave amplitude at distance r from the discharge channel axis, Pa); $P_{max00}$ is an initial pressure (pressure at the boundary of the discharge channel), Pa; $k_r$ is the geometric divergence coefficient (0.5 for cylindrical waves, 1 for spherical waves); r - distance from the discharge channel in the equatorial plane, m.

However, most of the above results were obtained for points

located in the equatorial plane of the discharge channel. In the case of the practical application of HVED, the pressure at points located at some distance from this plane is also of great interest. Determining the pressure at each point of the working space will improve the efficiency of various applications of the DPT and expand the scope of their application.

Now, experimental and theoretical research on the generation and propagation of pressure waves in liquids continues. The study of pressure wave propagation in a liquid during HVED can be approached through experimental or theoretical methods.

Properly designed experiments can yield results with minimal assumptions, closely resembling real-world DPT conditions. However, laboratory experiments on HVED often utilize various discharge chambers [11, 12], which allow for pressure measurements only at limited points-often a single location on the chamber wall, typically in the equatorial plane of the discharge channel. Experimentally solving this issue requires additional research, potentially involving modifications such as a discharge chamber with different dimensions, new fixtures for sensor placement, or multiple pressure sensors. These adjustments demand additional time and resources.

In contrast, theoretical approaches do not require additional experimental equipment. Using numerical modeling and/or semi-empirical formulas, theoretical methods can determine the amplitude of the pressure wave at any distance from the disturbance source and at any point in the study domain. However, theoretical results must be validated against experimental data.

Considering these factors, the research methodology will be to use a theoretical method to study the spatial propagation of pressure waves in fluid during HVED. In the study, we used semi-empirical expressions (semi-empirical model) and numerical modeling (mathematical model).

A semi-empirical model includes laws and an equation that was derived using experimental data. Thus, despite the use of a theoretical approach, experimental data will be used.

The mathematical model includes equations describing electrical and hydrodynamic processes during HVED in the discharge channel and the surrounding liquid.

Both models allow, independently of each other, the determination of the amplitudes of the pressure wave at different distances from the HVED source, both in the equatorial and non-equatorial planes. A comparison of the results obtained by the two methods will allow us to evaluate their accuracy and the possibility of their application for solving practical and scientific problems.

The primary aim of this study is to analyze the spatial propagation of pressure waves generated by HVED in water by using and comparing two independent modeling approaches-a semi-empirical method based on experimental data and a physics-based numerical simulation model. The goal is to establish reliable predictive equations for pressure amplitude at arbitrary points in both equatorial and off-equatorial planes of the discharge channel.

The specific objectives of the research are as follows:

- To construct a semi-empirical model for predicting pressure amplitudes based on existing experimental data and spatial geometric relationships;
- To implement a numerical model simulating the HVED-induced pressure field using a two-dimensional wave equation coupled with discharge circuit dynamics;
- To validate both models against each other and reference experimental results at various distances and angles from the discharge channel;
- To quantify the propagation behavior of pressure waves in different spatial directions and determine the practical applicability of both models in real DPT (discharge-pulse technology) scenarios.

## 3. INVESTIGATION OF PRESSURE WAVE PROPAGATION USING SEMI-EMPIRICAL EXPRESSIONS

The semi-empirical model can be conditionally divided into two parts. The first part considers the change in the amplitude of the pressure wave with distance from the source of action in the equatorial plane to the discharge channel. The second part considers the region of space outside the equatorial plane.

To solve the first part, we will use the known laws of propagation of changes in the parameters of the pressure wave during HVED described earlier.

Using (1) for two points in space 1 and 2, which are located at different distances from the source of the HVED:

$$P_{max2}/r_2^{-k_r} = P_{max1}/r_1^{-k_r} \quad (2)$$

Accordingly, if we know the amplitude of the pressure wave at some distance from the discharge channel in the equatorial plane, we can determine the amplitude of the pressure wave at another distance from the discharge channel (3) in this plane.

$$P_{max2} = P_{max1} r_2^{-k_r}/r_1^{-k_r} \quad (3)$$

Thus, to estimate the pressure wave amplitudes in the equatorial plane relative to the discharge channel, it is sufficient to have a single value at a known distance from the source. This value can be obtained using known analytical dependencies (some of which are provided in the review article [23]) or through experimental studies. A more accurate result will be obtained when using experimental data. Therefore, when carrying out our research, we used the results of a previously conducted experiment.

Smirnov et al. [12] measured the pressure wave amplitude generated by an electric discharge in a liquid using a physical model of a well casing with a diameter of 0.12 m (with the distance from the disturbance source to the measurement point being 0.06 m). The parameters were identical to those of an electro-discharge device for well decollmatization [24]: Capacitor bank capacity of 2.3 μF, discharge circuit inductance of 0.9 μH, charging voltage of 30 kV, discharge circuit resistance 0.08Ohm, and an interelectrode gap length of 0.025 m. The measured pressure wave amplitude was 37.3 MPa.

Using this value, the distribution of pressure wave amplitudes at different distances from the disturbance source was obtained (Figure 3). The experimental pressure measurement point was located within the cylindrical wave propagation zone. In this case, the transition from cylindrical to spherical symmetry occurs at a distance of 0.0625 m. Accordingly, to determine pressure amplitudes at a greater distance, the pressure at the transition boundary must be used (which was determined using (3) and found to be 36.55 MPa).

Analysis of the obtained data (Figure 3) showed that the pressure wave propagation in the equatorial plane relative to the discharge channel can be approximated by a power law

(the equation is shown in Figure 3), where the pressure wave amplitude decreases proportionally to distance as $r^{-0,72}$. This is in good agreement with the results from [18].

The pressure wave amplitudes in the non-equatorial plane relative to the discharge channel were experimentally investigated by Smirnov [14] (the measurement point scheme is shown in Figure 4). It was noted that at $\varphi=\pi/2$, the pressure wave amplitude decreases to $0.2P_{max0}$, where Pmax0 is the pressure wave amplitude in the equatorial plane.

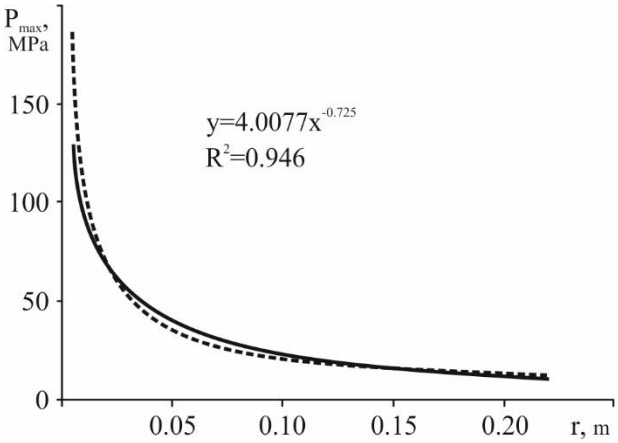


**Figure 3.** Pressure wave amplitudes at different distances from the disturbance (dotted line-trend line)

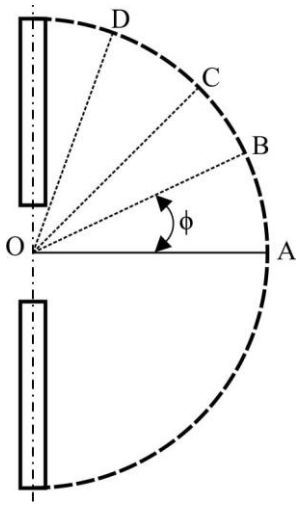


**Figure 4.** Measurement points [14]

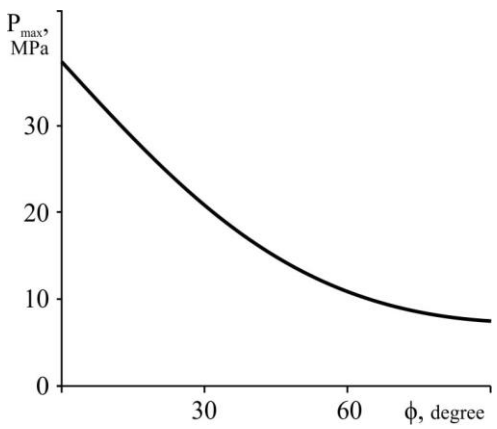


**Figure 5.** Pressure wave amplitude deviation from the equatorial plane (radius vector length 0.06 m)

A quadratic approximation (4) was provided for the experimental data obtained [13, 14], which satisfactorily describes the reduction of pressure wave amplitudes as they move away from the equatorial plane: OA-equatorial plane to the discharge channel; B, C, D-measurement points.

$$P_{max}(\varphi) = P_{max0} \cdot \left[\frac{3,2}{\pi}|\varphi| \cdot \left(\frac{|\varphi|}{\pi} - 1\right) + 1\right] \quad (4)$$

where, $\varphi$ is the angle between the radius vector of the considered point and the equatorial plane, rad; $P_{max0}$ is the pressure wave amplitude in the equatorial plane relative to the discharge channel, Pa; $P_{max}$ is the pressure wave amplitude, Pa.

The calculated pressure wave amplitudes when deviating from the equatorial plane using (4) for r=0.06 m and the known pressure at this point are shown in Figure 5.

Using Eqs. (3) and (4), we can determine the amplitude of the pressure wave at point B (Figure 2) using the following algorithm. Point B is located at the end of segment OB, which deviates from the equatorial plane by an angle of $\varphi$. To determine it, we first need to know the pressure at a distance OB from the discharge channel in the equatorial plane to the discharge channel.

Therefore, at the first stage, the length of segment OB is determined using (5):

$$OB = OA / \cos\varphi \quad (5)$$

Using Eq. (3), we determine the amplitude of the pressure wave at a distance OB from the discharge channel in the equatorial plane to the discharge channel. Knowing this pressure, we calculate the amplitude of the pressure wave at point B, which deviates from the equatorial plane by an angle of $\varphi$, using Eq. (4).

Figure 6 presents the distribution of pressure wave amplitudes along a normal to the equatorial plane of the discharge channel at a distance of 0.06 m from the disturbance source. The spatial coordinate $Y$ (the vertical distance from the equatorial plane to the considered point AB in Figure 2) was calculated using (6):

$$Y = AB = OA \cdot \mathrm{tg}\,\varphi \quad (6)$$

The analysis of the results showed that the dependence of the amplitudes of the pressure waves at a certain distance from the equatorial plane of the discharge channel along the normal to it (Y in the range from 0.01 m to 0.34 m) can be approximated by a power law (Figure 6(b) shows the equation of the dependence and the approximation reliability coefficient $R^2$).

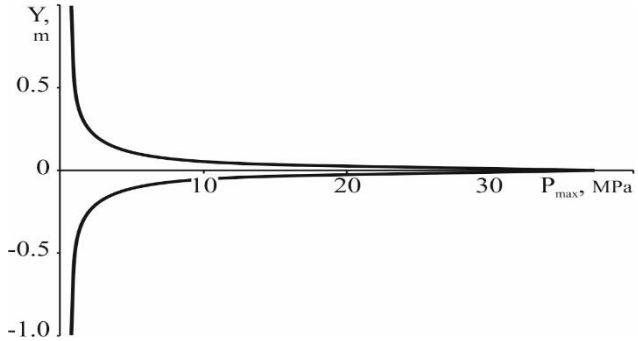


(a) Distribution of the pressure wave amplitude in two directions from the equatorial plane

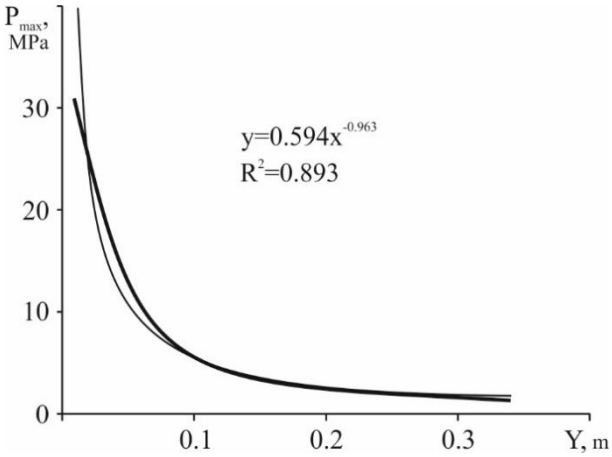

(b) Approximated by a power law (thin line - trend line)

**Figure 6.** Pressure wave amplitude distribution along the normal to the equatorial plane of the discharge channel at a distance of 0.06 m from the discharge channel

This approach allows for obtaining a family of curves (identical to the one in Figure 6(a)), which can be used to assess the effectiveness of electro-discharge impact on an object at any point in the working space, provided that the compressive strength limit of the object is known. If the incident pressure wave's amplitude exceeds the target object's strength limit, its destruction can be confidently predicted.

The calculations for this model used experimental results, which increases its accuracy. The equations used are simple, and the calculations do not require special software. The disadvantage of this approach is the need to know the amplitude of the pressure wave at least at one distance from the discharge channel.

## 4. NUMERICAL MODELING OF PRESSURE WAVE PROPAGATION DURING ELECTRO-DISCHARGE PROCESSES IN LIQUIDS

To study the propagation of pressure waves generated by the electric discharge process in a liquid, the mathematical model from Smirnov et al. [25] was taken as a basis. Testing of this model, including comparison with the results of experimental studies [26], showed good agreement between the calculation results and the reference data.

The mathematical model has a block structure and will consist of two blocks. The first block of the model describes the processes in the discharge circuit and the discharge channel. The second block describes the process of pressure wave propagation in the liquid.

When constructing the mathematical model, the following assumptions were made:

- At the initial moment, the discharge channel has the shape of a straight circular cylinder, the length of which is equal to the length of the interelectrode gap;
- The calculated space is filled with an ideal (non-viscous) liquid;
- Wave processes in the discharge channel can be neglected;
- The sizes of cavitation bubbles in the volume of liquid can be neglected.

The processes occurring in the discharge circuit and discharge channel are described by the equations [27]:

- The voltage balance in the discharge circuit Eq. (7);
- The energy balance in the discharge channel Eq. (8);
- The hydrodynamic equation establishing the relationship between the pressure in the discharge channel and the kinematic characteristics of its contact boundary (9);
- The Eq. (10) determines the relationship between the resistance of the discharge channel and the specific electrical conductivity of the plasma.

The propagation of the pressure wave in the liquid is described by the two-dimensional wave Eq. (11) [25, 28], a one-dimensional wave equation was used).

$$L\frac{dI}{dt} + I(R_{ch} + R_c) + \frac{q_e}{C} = U_0 \tag{7}$$

where, $I = dq_e/dt$.

$$\frac{d(p_{ch}S_{ch})}{dt}\frac{1}{\gamma - 1} + p_{ch}\frac{dS_{ch}}{dt} = I^2 R_{ch}\frac{1}{l} \tag{8}$$

$$p_{ch} = \frac{\rho_0}{2\pi}\frac{d^2 S_{ch}}{dt^2} ln\left(\frac{\pi^{0,5} l}{S_{ch}^{0,5}}\right) - \frac{\rho_0}{8\pi S_{ch}}\left(\frac{dS_{ch}}{dt}\right)^2 \tag{9}$$

$$R_{ch} = \frac{Al(\gamma - 1)}{p_{ch}S_{ch}} \tag{10}$$

$$\frac{\partial^2 \varphi_s}{\partial r_d^2} + \frac{1}{r_d}\frac{\partial \varphi_s}{\partial r_d} + \frac{\partial^2 \varphi_s}{\partial z^2} = \frac{1}{c_f^2}\frac{\partial^2 \varphi_s}{\partial t^2} \tag{11}$$

In Eqs. (7)-(11): $I$-discharge current, $A$; $L$-circuit inductance, $H$; $C$-capacitance of the capacitor bank, $F$; $U_0$-initial voltage at the start of the channel phase, $V$; $R_{ch}$-resistance of the discharge channel, $\Omega$; $R_c$-resistance of the circuit discharge, $\Omega$; $q_e$-electric charge, $C$; l-interelectrode distance, m; $p_{ch}$-pressure in the discharge channel, Pa; $S_{ch}$-cross-sectional area of the discharge channel, m²; $\gamma$-effective adiabatic index of the plasma in the channel ($\gamma$=1.26); $\rho_0$-density of the stationary liquid, kg/m³; $A$-spark constant (in our case $A=10^5$), $V^2 \cdot s \cdot m^{-2}$; $t$ - time, s; $\varphi_s$-velocity potential of the fluid motion, m²/s; $r_d$, z-spatial coordinates, m; $c_f$-speed of sound in the fluid, m/s.

The relationship between pressure in the liquid and the velocity potential is given by:

$$P = -\rho\frac{\partial \varphi_s}{\partial t} \tag{12}$$

where, is ρ-liquid density, kg/m³; $P$-pressure in the liquid, Pa.

The following boundary conditions are adopted:

- Equality of pressures in the discharge channel and the liquid at the interface;
- We consider the boundaries of the liquid space (calculation space) to be rigid. The condition of non-flow is applied to them.

At the initial moment, the liquid in the working (calculated) space is not disturbed.

The dimensions of the working space are taken from the calculation of the absence of influence of reflected waves on the results of modeling at the selected points.

The system of Eqs. (7)-(10) was solved using the Euler-Cauchy method, while the wave Eq. (11) was solved using the explicit cross method.

Preliminary, the model was tested for its ability to determine the pressure in the working space of the liquid by comparing the calculation results with experimental data. For this, the results of the article [24] were used. The initial calculation parameters corresponded to the parameters of the electric

discharge device used for cleaning wells: the capacity of the capacitor bank is 2.3 μF, the circuit inductance is 0.9 μH, the charging voltage is 30 kV, the discharge circuit resistance 0.08 Ohm, and the length of the interelectrode gap is 0.025 m. A pressure wave propagates in water: the speed of sound is 1500 m/s, and the density is 1000 kg/m$^3$.

Comparison of the calculated and experimental results in the equatorial plane to the discharge channel at a distance of 0.06 from the discharge channel showed their satisfactory coincidence (deviation<5%): the experimentally obtained pressure wave amplitude is 37.3 MPa, the pressure wave amplitude calculated by (7-11) is 38.89 MPa.

Subsequently, using the model (7-11), a study was made of the propagation of pressure waves in the liquid during the electric discharge process.

The results of numerical modeling (Figures 7 and 8) are in qualitative agreement with the conclusions of other authors [18] and with analytical calculations based on Eqs. (3)-(6). The propagation of the pressure wave in the equatorial plane (Figure 7) towards the discharge channel can be described by a power-law dependence, with the wave amplitude decreasing proportionally to the distance as $r^{-0.74}$.

Figure 8 shows the distribution of the pressure wave amplitude along the normal to the equatorial plane of the discharge channel at different distances from the discharge channel (for different values of $r$). Each distribution curve can be approximated by a power-law function with a satisfactory determination coefficient $R^2$. The study covered distances from 0.01 m to 0.15 m, and the obtained approximating expressions are given in Table 1.

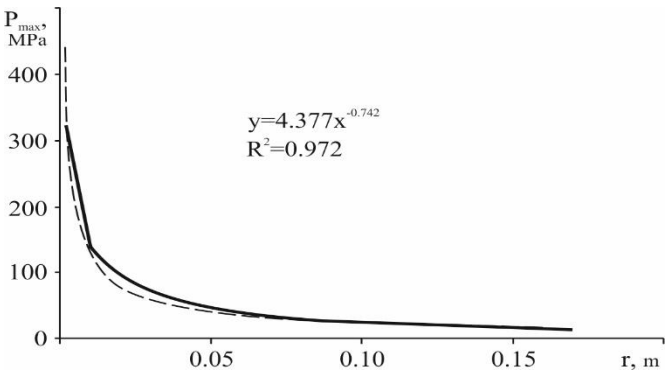


**Figure 7.** Propagation of a pressure wave in the equatorial plane calculated using a mathematical model (dotted line - trend line)

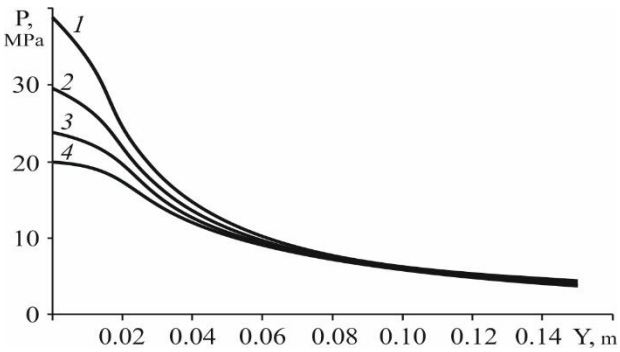


**Figure 8.** Distribution of the pressure wave amplitude on the normal drawn to the equatorial plane of the discharge channel: 1–$r$=0.06 m; 2–$r$=0.08 m; 3–$r$=0.1m; 4–$r$=0.12 m

**Table 1.** Approximating expressions for the amplitude distribution of the pressure wave along a normal to the equatorial plane of the discharge channel

| *r, m* | *P(Y)* | $R^2$ |
|---|---|---|
| 0.06 | $P$=0.973$Y^{-0,813}$ | 0.965 |
| 0.08 | $P$=1.097$Y^{-0,749}$ | 0.944 |
| 0.1 | $P$=1.215$Y^{-0,693}$ | 0.919 |
| 0.12 | $P$=1.333$Y^{-0,643}$ | 0.895 |

An analysis of the data presented in Table 1 shows that with increasing distance $r$, the exponent in the power function decreases.

The advantage of numerical modeling is the ability to obtain a wave pattern in the entire workspace in one modeling cycle. However, its application requires appropriate software. This is not always possible in practical applications of HVED.

## 5. COMPARISON OF THE RESULTS OF TWO CALCULATION APPROACHES USED IN THIS WORK

Sections 3 and 4 present two models for solving the same problem that are essentially different. Therefore, one way to test them is to compare their results with each other.

For testing, we chose the mode that has already been used in this work: the capacity of the capacitor bank is 2.3 μF, the circuit inductance is 0.9 μH, the discharge circuit resistance 0.08 Ohm, the charging voltage is 30 kV, the length of the interelectrode gap is 0.025 m.

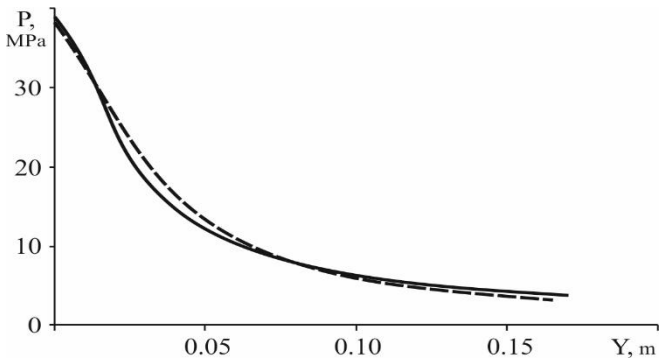


**Figure 9.** Distribution of pressure wave amplitude along the normal to the equatorial plane of the discharge channel: solid line-model (7-11); dashed line-model (3-6)

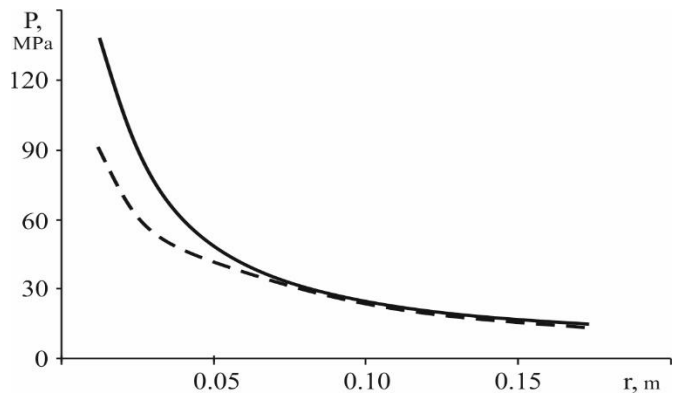


**Figure 10.** Distribution of pressure wave amplitude in the equatorial plane of the discharge channel: solid line-model (7-11); dashed line-model (3-6)

For calculations based on expressions (3-6), it is necessary to know the pressure values at a known distance from the discharge channel. Therefore, to maintain the identity of all initial conditions for the two models, it was assumed that at $r$=0.06 m, the pressure amplitude in the equatorial plane of the discharge channel is $P_{max0}$=38.89 MPa. This pressure was obtained by solving the mathematical model (7-11).

Comparison of the calculation results for the two models at points outside the equatorial plane to the discharge channel (normal to it, at a distance of 0.06m from the discharge channel) showed satisfactory qualitative and quantitative matching (Figure 9). In the zone (up to Y=0.17 m), the difference between the results was less than 20%.

Comparison of the pressure wave amplitude distribution in the equatorial plane (Figure 10) to the discharge channel showed good qualitative agreement of the results. At a distance of r>0.05 meters, satisfactory quantitative matching can be noted (the discrepancy is less than 11%). As the discharge channel is approached, the discrepancy of the results increases, and at a distance of 0.01 meters is about 40%. Most likely, this is because in real conditions, with HVED in liquid, a deviation of the pressure wave propagation law from cylindrical is observed in the near zone to the discharge channel. This assumption is consistent with the results given by Sayapin et al. [29].

Comparison of the calculation results for the two models showed satisfactory qualitative and quantitative matching of the results, both in the equatorial plane of the discharge channel and outside it. This, as well as the results of other testing, allows us to assert that these models can be used to solve scientific and practical problems related to the propagation of a pressure wave in a liquid during an HVED.

## 6. PROSPECTS FOR FUTURE RESEARCH

The authors plan to continue studying pressure waves in HVED, both experimentally and theoretically. For example, future theoretical studies that will continue the topic of this work will be devoted to:

- Considering the effect of liquid;
- Applying more complex boundary conditions that will consider the complex geometry of the working space and the electrode system.

This study assumes linear wave propagation. However, real conditions in HVED can be accompanied by nonlinearities (for example, in some HVED modes, shock waves can form). Therefore, future studies will also focus on considering the nonlinear behavior of waves to obtain a more accurate wave pattern.

Another possible direction for improving the mathematical model is its expansion to a three-dimensional form. This will allow for more detailed consideration of the influence of boundary conditions.

## 7. CONCLUSIONS

This study presents a comprehensive analysis of pressure wave propagation in liquids during HVED, utilizing both semi-empirical and numerical modeling approaches. Unlike most existing research focused solely on equatorial planes or based on a single methodology, this work investigates spatial pressure distribution in both equatorial and off-equatorial directions using two fundamentally different models.

Key findings:

- Both modeling approaches predict that pressure wave amplitude in the equatorial plane decays according to a power law, with exponents ranging from –0.72 (semi-empirical) to –0.74 (numerical).
- In the off-equatorial direction, pressure amplitude can also be described by a power function, with decreasing exponent as the radial distance increases.
- The comparison of both models showed satisfactory agreement, with less than 11% deviation in the equatorial plane (for r>0.05 m) and less than 20% deviation in the off-equatorial region.

The semi-empirical model is simple to implement, requires no specialized software, and is highly effective when at least one pressure measurement is available. This makes it suitable for quick assessments in field applications. However, its accuracy depends on experimental input, and it assumes simplified wave behavior, limiting its use in complex geometries.

The numerical model, in contrast, allows for detailed, high-resolution simulation of pressure fields across the entire workspace. It is self-contained and can simulate arbitrary geometries and boundary conditions, making it well-suited for research and design purposes. Its limitations include computational cost and sensitivity to modeling assumptions such as ideal fluid behavior.

The developed models are relevant for various discharge-pulse technology (DPT) applications where pressure wave control is critical. For example, in well cleaning, predicting the pressure amplitude at different points enables optimization of discharge energy to maximize sediment removal without damaging well structures. In rock fragmentation, knowing the spatial pressure distribution improves efficiency and safety. In medical contexts, such as lithotripsy, accurate modeling ensures targeted energy delivery while minimizing collateral effects.

The semi-empirical model can be applied in practical environments with limited measurement capabilities, while the numerical model is valuable for design optimization and theoretical analysis.

Future studies will aim to improve model fidelity by:

- Incorporating fluid viscosity and nonlinear wave effects (e.g., shock wave formation);
- Introducing more realistic boundary conditions and complex geometries;
- Extending the model to a fully three-dimensional framework;
- Performing targeted experiments to validate predictions in non-equatorial planes.

While the primary focus of this work has been on the development and validation of theoretical and semi-empirical models, the practical application of these models remains a key direction for future research. Building on the spatial pressure distributions established here, future studies will apply the developed models to specific industrial scenarios, including well stimulation, rock disintegration, and medical applications such as lithotripsy. These efforts will involve coupling the modeling approaches with real-world geometries, material properties, and boundary conditions to support the optimization of DPT systems in operational environments.

## REFERENCES


[1] Liu, Q., Zhang, Y. (2014). Shock wave generated by high-energy electric spark discharge. Journal of Applied Physics, 116(15): 153302. https://doi.org/10.1063/1.4898141

[2] Higa, O., Matsubara, R., Higa, K., Miyafuji, Y., Gushi, T., Omine, Y., Naha, K., Shimojima, K., Fukuoka, H., Maehara, H., Tanaka, S., Matsui, T., Itoh, S. (2012). Mechanism of the shock wave generation and energy efficiency by underwater discharge. International Journal of Multiphysics, 6(2): 89-98. https://doi.org/10.1260/1750-9548.6.2.89

[3] Qiao, L., Zhang, X., Yan, B., Liu, Y., Han, Z. (2021). An underwater discharge shockwave separation method based on minimum-Phase cepstrum. AIP Advances, 11(9): 095109. https://doi.org/10.1063/5.0064322

[4] Banožić, M., Jozinović, A., Grgić, J., Miličević, B., Jokić, S. (2021). High voltage electric discharge for recovery of chlorogenic acid from tobacco waste. Sustainability, 13(8): 4481. https://doi.org/10.3390/su13084481

[5] Rizun, A.R., Denisyuk, T.D., Domershchikova, A.O. (2017). Electric discharge in the process for recovering the wastes of printed circuit boards. Surface Engineering and Applied Electrochemistry, 53(6): 592-596. https://doi.org/10.3103/S1068375517060096

[6] Sato, M., Sakugawa, T., Yamashita, T., Hosano, N., Hosano, H. (2020). Effects of voltage and current waveforms on pulse discharge energy transfer to underwater shock waves for medical applications. IEEE Transactions on Plasma Science, 48(7): 2639-2645. https://doi.org/10.1109/TPS.2020.2992638

[7] Chung, K.J., Lee, S.G., Hwang, Y.S., Kim, C.Y. (2015). Modeling of pulsed spark discharge in water and its application to well cleaning. Current Applied Physics, 15(9): 977-986. https://doi.org/10.1016/j.cap.2015.05.010

[8] Cai, Z., Zhang, H., Liu, K., Chen, Y., Yu, Q. (2020). Experimental investigation and mechanism analysis on rock damage by high voltage spark discharge in water: Effect of electrical conductivity. Energies, 13(20): 5432. https://doi.org/10.3390/en13205432

[9] Krivitsky, E.V., Shamko, V.V. (1979). Transient processes in high-voltage discharge in water. Naukova Dumka, Kyiv, 208.

[10] Touya, G., Reess, T., Pecastaing, L., Gibert, A., Domens, P. (2006). Development of subsonic electrical discharges in water and measurements of the associated pressure waves. Journal of Physics D: Applied Physics, 39(24): 5236-5244. https://doi.org/10.1088/0022-3727/39/24/021

[11] Smirnov, A.P., Zhekul, V.G., Taftai, E.I., Khvoshchan, O.V., Shvets, I.S. (2019). Effect of parameters of liquids on amplitudes of pressure waves generated by electric discharge. Surface Engineering and Applied Electrochemistry, 55: 84-88. https://doi.org/10.3103/S1068375519010149

[12] Smirnov, A.P., Zhekul, V.G., Mel'kher, Y.I., Taftai, E.I., Khvoshchan, O.V., Shvets, I.S. (2018). Experimental investigation of the pressure waves generated by an electric explosion in a closed volume of a fluid. Surface Engineering and Applied Electrochemistry, 54: 475-480. https://doi.org/10.3103/S1068375518050101

[13] Shamko, V.V., Kucherenko, V.V. (1991). Theoretical foundations of engineering calculations of energy and hydrodynamic parameters of underwater spark discharge. IIPT NAS of Ukraine, Mykolaiv, 52.

[14] Okun, I.Z. (1971). Investigation of compression waves arising from a pulse discharge in water. Journal of Technical Physics, 41(2): 292-301.

[15] Miyata, K., Ito, H. (2014). Propagation mode and pressure measurement of underwater shock wave by large current short-pulse discharge. Symposium on Frontiers of Applied Pulse Power Technology; Toki, Gifu (Japan), p. 1-6.

[16] Liu, Y., Li, Z., Li, X., Zhou, G., Li, H., Zhang, Q., Lin, F. (2017). Energy transfer efficiency improvement of liquid pulsed current discharge by plasma channel length regulation method. IEEE Transactions on Plasma Science, 45(12): 3231-3239. https://doi.org/10.1109/TPS.2017.2651105

[17] Chai, Y., Timoshkin, I.V., Wilson, M.P., Given, M.J., MacGregor, S.J. (2023). Free and wire-guided spark discharges in water: Pre-breakdown energy losses and generated pressure impulses. Energies, 16(13): 4932. https://doi.org/10.3390/en16134932

[18] Li, X., Chao, Y., Wu, J., Han, R., Zhou, H., Qiu, A. (2015). Study of the shock waves characteristics generated by underwater electrical wire explosion. Journal of Applied Physics, 118(2): 023301. https://doi.org/10.1063/1.4926374

[19] Yan, D., Wu, Q., Chen, I., Zhao, N. (2020). Analysis of shockwave front-time characteristics based on pulse discharge in water. Journal of Engineering Science & Technology Review, 13(4): 30-36. https://doi.org/10.25103/jestr.134.03

[20] Kanagawa, T., Ishitsuka, R., Arai S., Ayukai T. (2022). Contribution of initial bubble radius distribution to weakly nonlinear waves with a long wavelength in bubbly liquids. Physics of Fluids, 34(10): 103320. https://doi.org/10.1063/5.0099282

[21] Kanagawa, T., Ayukai, T., Kawame, T., Ishitsuka, R. (2021). Weakly nonlinear theory on pressure waves in bubbly liquids with a weak polydispersity. International Journal of Multiphase Flow, 142: 103622. https://doi.org/10.1016/j.ijmultiphaseflow.2021.103622

[22] Zhang, C., Hu, X., Adams, N.A. (2017). A weakly compressible SPH method based on a low-dissipation Riemann solver. Journal of Computational Physics, 335: 605-620. https://doi.org/10.1016/j.jcp.2017.01.027

[23] Smirnov, O.P. (2017). Methods for determining the parameters of the pressure wave generated by an electric discharge in a liquid. Geotechnical Mechanics, (136): 23-33.

[24] Zhekul, V.G., Litvinov, V.V., Mel'kher, Yu.I., Smirnov, A.P., Taftai, E.I., Khvoshchan, O.V., Shvets, I.S. (2017). Submersible electric discharge devices for the intensification of mining operations. Oil and Gas Power Engineering, (1): 23-31.

[25] Smirnov, A.P., Kosenkov, V.M., Zhekul, V.G., Poklonov, S.G. (2010). The study of the effect of the electrodischarge action modes on viscous deposits in cylindrical channels. Surface Engineering and Applied Electrochemistry, 46(3): 237-242. https://doi.org/10.3103/S1068375510030087

[26] Smirnov, A.P., Zhekul, V.G., Poklonov, S.G. (2011). Testing a mathematical model of the electrodischarge effect on viscous sediments. Surface Engineering and

Applied Electrochemistry, 47(2): 145-151. https://doi.org/10.3103/S1068375511020189
[27] Krivitsky, E.V. (1986). Dynamics of electrical explosion in liquids. Naukova Dumka, Kyiv, 208.
[28] Sverdlina, G.M. (1990). Applied Hydroacoustics. Shipbuilding, Leningrad, 320.
[29] Sayapin, A., Grinenko, A., Efimov, S., Krasik, Y.E. (2006). Comparison of different methods of measuring the pressure of underwater shock waves generated by electrical discharge. Shock Waves, 15(2): 73-80. https://doi.org/10.1007/s00193-006-0011-8

## NOMENCLATURE

| | |
|---|---|
| $A$ | spark constant, $V^2 \cdot s \cdot m^{-2}$ |
| $C$ | capacitance of the capacitor bank, F |
| $c_f$ | speed of sound in the fluid, m/s |
| $I$ | discharge current, A |
| $k_r$ | geometric divergence coefficient |
| $L$ | circuit inductance, H |
| $l$ | interelectrode distance, m |
| $P$ | pressure in the liquid, Pa |
| $p_{ch}$ | pressure in the discharge channel, Pa |
| $P_{max00}$ | initial pressure (pressure at the boundary of the discharge channel), Pa |
| $P_{max0}$ | is the pressure wave amplitude in the equatorial plane relative to the discharge channel, Pa |
| $P_{max}$ | pressure wave amplitude, Pa |
| $q_e$ | electric charge, C |
| $R^2$ | approximation reliability coefficient |
| $R_c$ | resistance of the circuit discharge, Ω |
| $R_{ch}$ | resistance of the discharge channel, Ω |
| $r$ | distance from the discharge channel in the equatorial plane, m |
| $r_d$ | spatial coordinates, m |
| $S_{ch}$ | cross-sectional area of the discharge channel, $m^2$ |
| $t$ | time, s |
| $U_0$ | initial voltage at the start of the channel phase, V |
| $Y$ | distance to the calculated point on the normal to the equatorial plane to the discharge channel, m |
| $z$ | spatial coordinates, m |

### Greek symbols

| | |
|---|---|
| $\gamma$ | effective adiabatic index of the plasma in the channel |
| $\rho$ | liquid density, $kg/m^3$ |
| $\rho_0$ | density of the stationary liquid, $kg/m^3$ |
| $\varphi$ | angle between the radius vector of the considered point and the equatorial plane, rad |
| $\varphi_s$ | velocity potential of the fluid motion, $m^2/s$ |

### Subscripts

| | |
|---|---|
| 1 | point number in the working (calculated) space |
| 2 | point number in the working (calculated) space |